Superpropulsion of Droplets and Soft Elastic Solids

Christophe Raufaste, Gabriela Ramos Chagas, Thierry Darmanin, Cyrille Claudet, Frédéric Guittard, Franck Celestini

▶ **To cite this version:**

Christophe Raufaste, Gabriela Ramos Chagas, Thierry Darmanin, Cyrille Claudet, Frédéric Guittard, et al.. Superpropulsion of Droplets and Soft Elastic Solids. Physical Review Letters, 2017, 119, pp.108001. 10.1103/PhysRevLett.119.108001 . hal-01584717

HAL Id: hal-01584717

https://hal.science/hal-01584717

Submitted on 9 Sep 2017

HAL is a multi-disciplinary open access archive for the deposit and dissemination of scientific research documents, whether they are published or not. The documents may come from teaching and research institutions in France or abroad, or from public or private research centers.

L'archive ouverte pluridisciplinaire **HAL**, est destinée au dépôt et à la diffusion de documents scientifiques de niveau recherche, publiés ou non, émanant des établissements d'enseignement et de recherche français ou étrangers, des laboratoires publics ou privés.

Superpropulsion of droplets and soft elastic solids

Christophe Raufaste,[1] Gabriela Ramos Chagas,[2] Thierry Darmanin,[2]
Cyrille Claudet,[1] Frédéric Guittard,[2] and Franck Celestini[1, *]

[1] *Université Côte d'Azur, CNRS, Institut de Physique de Nice, 06100 Nice, France*
[2] *Université Côte d'Azur, NICE Lab, IMREDD, 61-63 avenue Simone Veil, 06200 Nice, France*

(Dated: September 9, 2017)

We investigate the behavior of droplets and soft elastic objects propelled with a catapult. Experiments show that the ejection velocity depends on both the projectile deformation and the catapult acceleration dynamics. With a subtle matching given by a peculiar value of the projectile/catapult frequency ratio, a 250% kinetic energy gain is obtained as compared to the propulsion of a rigid projectile with the same engine. This superpropulsion has strong potentialities: actuation of droplets, sorting of objects according to their elastic properties and energy saving for propulsion engines.

PACS numbers:

Droplets are very specific objects owing to their interfacial properties [1]. They keep their integrity and shape at rest due to surface tension, but are very deformable and difficult to manipulate since they adhere to regular substrates. Nevertheless droplet motion can be triggered when the surface wetting properties are inhomogeneous: self-propulsion is thus observed when the substrate surface exhibits a gradient of free surface energy [2] or when a droplet itself triggers a contact angle difference between its leading and trailing edges [3, 4]. Their dynamical properties are at the origin of peculiar behaviors [5] and their vibration modes [6] can be forced in a way to control their motion over a substrate [7, 8] and to let them move against gravity [9]. The contact with the substrate can also be prevented by triggering the Leidenfrost effect [10, 11], which leads to nonsticky drops that move easily [12]. In the same vein, the development of superhydrophobic surfaces (SHSs) allows one to minimize the adhesion with the substrate [13] and droplets can bounce on such surfaces like elastic balls with a velocity restitution coefficient that depends on the relative importance of inertial and capillary effects [14]. Recently Boreyko and Chen [15] have studied the coalescence of droplets during vapor condensation on SHSs. The surface energy release associated with the coalescence is partly transformed into kinetic energy and induces a vertical propulsion of the merged drops.

In this letter we investigate the capillary-inertial behavior of droplets propelled by a catapult. To summarize, we first consider droplets launched with a simple spring catapult, the plate surface of which is superhydrophobic to prevent any adhesion. We show that the transfer of kinetic energy can be increased by 250% as compared to propelling rigid objects with the same engine. This superpropulsion phenomenon is obtained when the catapult is tuned to perform the ejection with a subtle matching between its own dynamics and the one of the projectile deformation. The same behavior is then experimentally recovered with soft elastic solids, demonstrating the generality of the phenomenon. The experimental results are in good agreement with a simple physical model and the optimal ejection is reached with a peculiar value of the projectile/catapult frequency ratio, different from the ones of classical resonant phenomena. Finally, several direct applications are discussed and illustrated in the conclusion.

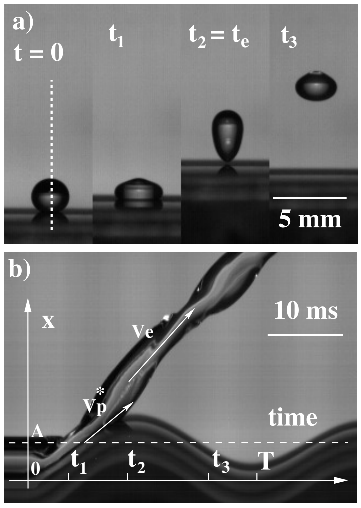

FIG. 1: a) Image sequences of a typical droplet propulsion standing on a SHS intially at rest at $t = 0$ (see movie M1[19]). In the initial stage of the droplet propulsion (t_1), the droplet deformation is not homogeneous but concentrated in its lower part. In an intermediate stage the deformation reaches the top of the droplet. Later on (t_e) the droplet leaves the catapult with a complex and deformed shape. During its flight (t_3), we clearly see the oscillation modes of frequency f_0. b) A space-time diagram is built along the dashed line drawn in image $t = 0$. It illustrates the oscillatory motion of the catapult plate and the difference between the maximum plate velocity and the ejection velocity of the droplet.

The experimental setup consists in a catapultlike engine built with a spring of variable stiffness. A similar setup was used by Clanet et al [16] to emphasize the droplet deformation under strong acceleration. The catapult is initially loaded and maintained at rest with an electromagnet. The initial distance between the plate and its equilibrium position can be varied and is typically of a few millimeters. Once the electromagnet is switched on, the plate is subject to a sudden and large acceleration, typically 10 times the gravity. The catapult plate is a SHS of high quality to prevent droplet adhesion. We use two different kinds of SHSs with ultralow hysteresis and sliding angle that are obtained by electropolymerization. The first one is a superhydrophobic and superoleophobic fluorinated poly(3,4-ethylenedioxypyrrole) [17] and the second one a superhydrophobic fluorinated polyfluorene [18]. Their low hysteresis and sliding angles, less than 2.0 degrees, are due to the combination of microstructures and nanostructures/nanoporosities with the low surface energy of the fluorinated chains. Indeed we have demonstrated and discussed in ref. [17] how the presence of nanoporosities is crucial to highly reduce the water adhesion on the surface.

Droplets are propelled with this device and the ejection dynamics is imaged by a high-speed camera with frame rates ranging from 500 to 5000 fps. Snapshots of the main steps of a drop ejection are given in Fig. 1a: the drop is represented, first at rest on the SHS, second during the initial acceleration of the plate, third at the take-off time t_e and finally during its flight. For each ejection, a space-time diagram is built along a vertical line passing through the center of the droplet (Fig. 1b). It displays both the plate and the droplet motion as functions of time. We have checked that the plate motion is harmonic. Its period $T = 1/f$ and amplitude A are directly measured from the diagram, as well as its maximum velocity V_p^*, which corresponds to the plate velocity when it reaches its equilibrium position at $T/4$. The drop ejection velocity V_e and the takeoff time t_e are also determined using the space-time diagram. We can also see in Fig. 1b (and in movie M1 [19]) that, during its flight after takeoff, the drop experiences oscillations that we used to measure its eigenfrequency f_0. We have checked that these measurements are in agreement with the surface tension driven oscillation modes of droplets, *i.e* $f_0 \propto R^{-3/2}$ [6], R being the radius of the drop.

Experiments were performed with droplet radii ranging between 0.5 and 1.8 mm and catapult frequencies between 20 and 70 Hz . For a given droplet radius and a given catapult frequency, a linear regime is found and characterized by the ejection velocity V_e proportional to the load amplitude A. At low amplitude, the adhesion with the substrate cannot be neglected anymore and the ejection is less efficient. At large amplitude, the velocity is smaller than expected as well, which seems related to the nonlinear response of the drop (large deformation and/or fragmentation) to strong solicitations.

In what follows, we always work in the linear regime and characterize the ejection efficiency by the energy transfer factor $\alpha = (V_e/V_p^*)^2$. This coefficient characterizes the gain or loss of kinetic energy as compared to the ejection of a rigid projectile that is expected to takeoff from the substrate with $V_e = V_p^*$ or $\alpha = 1$. We performed several experiments varying the size of the drop while keeping constant the catapult frequency. We can see that in most cases, the droplets are ejected with a velocity larger than the one expected for a rigid projectile and that α depends significantly on the droplet size (Fig. 2). By varying both the droplet radius and the catapult frequency in our experiments, we found that all data collapse by plotting α as a function of the drop/catapult frequency ratio f_0/f (Fig. 3). Around $f_0/f \sim 3$, α reaches maximal values close to roughly 2.5. Note that α quantifies only the translational kinetic energy of the system. In fact, the droplets exhibit more or less pronounced oscillations after takeoff emphasizing that some energy is transferred to the projectile to stimulate modes as well.

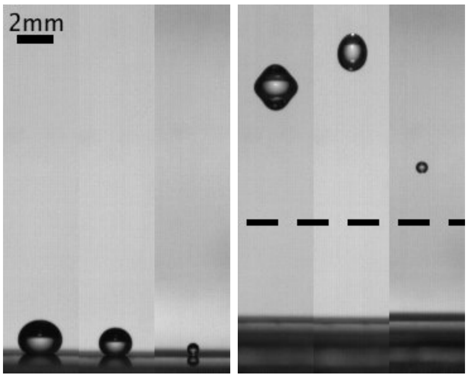

FIG. 2: The figure displays snapshots of three experiments performed with several drop sizes and the same catapult characteristics ($f = 37$ Hz and $A = 1.4$ mm), see movie M1 [19]. Left: Position before the motion initiation. Right: Vertical position reached after ejection once all the kinetic energy is transferred into gravitational potential energy. The dashed line indicates the position that would reach the center of mass of a rigid object.

We also measure the time t_e at which the droplet is ejected. Again, a unique trend is found when plotting t_e/T as a function of f_0/f. Most of the values are larger than 0.25, the value expected for a rigid projectile because of the plate deceleration. The smaller the f_0/f ratio, the longer the contact during the deceleration phase.

We now consider the ejection of hydrogel balls by the same spring catapult. These balls are composed of polyacrylamide, a water-absorbing polymer, and can be found in any regular flower shop. They are initially dry with a radius of 1mm and their final radius ranges between 5 and 10 mm depending on the hydration time in a water bath. The Young modulus of this material is known to be a decreasing function of the hydration

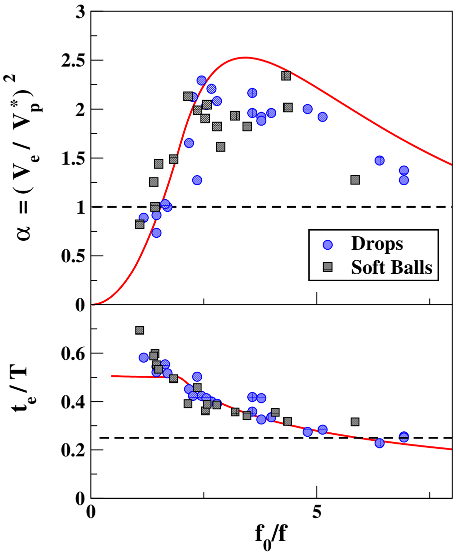

FIG. 3: The figure summarizes measurements performed with both droplets (circles) and hydrogel balls (squares). Top: Energy transfer factor α plotted as a function of the frequency ratio f_0/f. The dashed line represents $\alpha = 1$, the value expected for a rigid projectile, while the model based on the projectile deformation dynamics is represented by the solid line. Bottom: Same data and analysis for t_e/T as a function of f_0/f. The dashed line represents $t_e/T = 0.25$, the value expected for a rigid projectile.

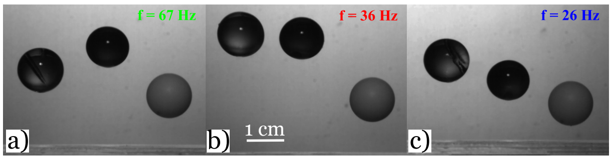

FIG. 4: The figure displays the simultaneous propulsion of soft elastic balls for several catapult frequencies (see movies M2, M3 and M4 [19]). The two first projectiles are hydrogel balls of eigenfrequency $f_0 = 90$ and 150 Hz respectively. The right-most ball is rigid.

time and typically ranges between 2 and 20 kPa. We have experimentally measured eigenfrequencies between 50 and 200 Hz. Experiments are performed for several catapult frequencies as well and the results are superimposed to the former ones obtained with the droplets (Fig. 3). The same trends are recovered for α and t_e/T as functions of f_0/f. Again, the superpropulsion is observed with α values significantly higher than one. As illustrated in Fig. 4, by tuning the catapult frequency, we can choose the hydrogel ball that we want to propel the most efficiently.

We clearly demonstrate the generality of the phenomenon observed for these two different systems. We can therefore infer that the phenomenon is related to the deformation dynamics of the projectile: it is triggered by surface tension for the droplets and by elasticity for the soft balls. The peculiar value of the maximal efficiency reached with $f_0/f \sim 3$ differs from the ones of classical resonant phenomena: respectively 1 and 2 for driven harmonic and parametric oscillators. This suggests to adopt the most basic approach and to solve the wave equation for the projectile deformation with the peculiar boundary conditions imposed by the catapult propulsion.

The substrate is initially considered at rest at the position $x = 0$. At $t = 0$, it initiates an harmonic motion given by $U_s(t) = A(1 - \cos(2\pi f t))$. The velocity $V_p(t) = dU_s(t)/dt$ reaches its maximum value $V_p^* = 2\pi f A$ at $T/4$ (Fig. 5). These values correspond respectively to the ejection velocity and take-off time for a rigid object standing on the substrate without adhesion. The plate decelerates between $T/4$ and $T/2$, and recesses after $T/2$. The projectile extends initially from $x = 0$ to $x = 2R$ and is simply modeled as a 1D elastic material. We assume linear elasticity and the wave equation derives from Hooke's law [20]. Denoting $u(x, t)$ the displacement of an element at a time t that was initially found at the position x, the wave equation is written as

$$\frac{\partial^2 u}{\partial t^2} = c^2 \frac{\partial^2 u}{\partial x^2}, \tag{1}$$

with c the propagation velocity. Three boundary conditions are applied. First, the projectile is initially at rest without any deformation ($u(x, 0) = 0$). Second, the projectile displacement at the bottom is driven by the substrate motion ($u(0, t) = A(1 - \cos(2\pi f t))$). Finally the local deformation on the top is fixed to zero to account for the free end (Neumann boundary condition $\frac{\partial u}{\partial x}(2R, t) = 0$). It is important to note that no dissipation term is included in the equation. We have verified that both inertial and capillary effects are dominant against viscous ones by estimating the Reynolds and capillary numbers. Eq. 1 can be set under a dimensionless form by taking $1/f$ and $2R$ as time and length scales: it shows that the dynamics is a unique function of the ratio of two time scales, the catapult acceleration time and the traveling time of a perturbation propagating back and forth inside the object. It is worth noticing that the latter corresponds to the fundamental period $T_0 = 4R/c$ of the projectile. In the following, we use the dimensionless parameter $f_0/f = T/T_0$ for convenience.

The wave equation is solved numerically for a set of f_0/f values by a finite difference scheme. Each simulation is stopped when the projectile loses its contact with the substrate ($\frac{\partial u}{\partial x}(0, t_e) = 0$), defining the ejection time t_e. The average velocity of the projectile V_e is then computed and used to calculate the energy transfer factor α.

The agreement between the model and the experiments is very good without any free parameter (Fig. 3). The parameter α exhibits a maximum of 2.5 around $f_0/f = 3.4$, very close to the values found experimentally. The theoretical prediction for t_e/T is also very satisfactory. For small f_0/f values, the model predicts a saturation value $t_e = T/2$ corresponding to the recessing time of the plate, which is not observed in the experiment. This slight disagreement is probably due to the simplicity of the 1D model geometry compared to the spherical shape of droplets and hydrogel balls.

This model helps to reach a physical interpretation of the phenomenon. The key point is that the ejection velocity at t_e is the sum of two different quantities: first the velocity of the plate, $V_p(t_e)$, second the velocity of the center of mass of the projectile in the frame of reference of the plate, $V_{cm}(t_e)$. The velocity $V_p(t)$ is initially positive and an increasing function between $t = 0$ and $t = T/4$ at which it reaches the maximum V_p^* before decreasing. The projectile is initially in a compression phase, so that the velocity $V_{cm}(t)$ is negative and decreases with time to reach a negative maximum. It then enters an extension phase reaching a positive maximum. The transition between the compression phase ($V_{cm} < 0$) and the extension phase ($V_{cm} > 0$) is related to both T and T_0. It ranges between T_0 (more rigid projectiles) and $T/2$ (softer projectiles). The superpropulsion phenomenon is therefore obtained when a subtle matching between T and T_0 is obtained for the maximization of $V_e(t_e) = V_p(t_e) + V_{cm}(t_e)$ with an ejection time t_e at which the reaction force on the plate is 0. This is illustrated in Fig. 5a where we plot $V_p(t)$, $V_{cm}(t)$ and $V_e(t)$ for three different cases. For a soft material (e.g. $f_0/f = 0.5$) the velocity of the plate at $t = t_e$ equals zero and the only contribution to $V_e(t_e)$ comes from $V_{cm}(t_e)$. For a rigid projectile (e.g. $f_0/f = 7$) at $t = t_e$, the plate velocity is large but the contribution from $V_{cm}(t_e)$ is not significant at all. The best ejection is therefore obtained in an intermediate situation ($f_0/f = 3.4$) where the projectile is propelled with a significant velocity coming equally from the motion of the plate and the center of mass of the projectile. This point is illustrated in Fig. 5b where we plot the velocities $V_p(t_e)$, $V_{cm}(t_e)$ and $V_e(t_e)$ as functions of the frequency ratio f_0/f.

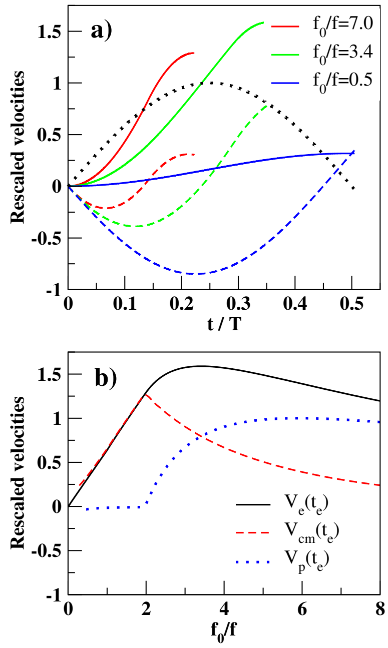

FIG. 5: a) Plate velocity $V_p(t)$ (dotted line), center of mass velocity in the reference frame of the plate $V_{cm}(t)$ (dashed lines) and ejection velocity $V_e(t)$ (solid lines) as functions of time for three frequency ratios. b) V_p, V_{cm} and V_e at the ejection time t_e as functions of f_0/f. All velocities are rescaled by the the maximal plate velocity $V_p^* = 2\pi f A$.

In this communication we have evidenced an unexpected behavior of droplets and soft elastic projectiles launched by a catapultlike engine. Depending on the frequency ratio between the dynamics of the projectile and the one of the catapult, the transfer of kinetic energy can be increased by a factor 2.5 as compared to the case of a rigid object. The experiments are in very good agreement with a simple physical model accounting for the deformation dynamics of the projectile. The model emphasizes the generality of this physical mechanism and its close connection to the classical phenomenon of resonance. The superpropulsion could thus be viewed as a "one-shot resonance".

Besides the fundamental interest, we envisage direct applications in various domains. As illustrated in the movie M1 [19], drops can be sorted by size by tuning the catapult frequency at the desired value. To our knowledge it is also the first evidence of an accurate drop actuation in the vertical direction. In the same vein, we have verified that a simple device can sort objects according to their elastic properties (movies M2, M3 and M4 [19]). Experiments presented in this communication have been realized with SHSs without any significant adhesion. This is not the case for all SHSs and the ejection phenomenon could be used to dynamically characterize the substrates. We are actually performing experiments to quantitatively measure the robustness of the Cassie-Baxter state against the Wenzel one. Finally, we expect new possibilities to save energy in ballistics technologies or to improve the efficiency of propelling engines by tuning not only the deformation properties of the projectile but also the ones of the propelling engine itself.

We thank T. Frisch, J. Mathiesen and S. Dorbolo for fruitful discussions. This work was partially supported by CNPq, Conselho Nacional de Desenvolvimento Científico e Tecnológico - Brazil (Process N° 202280/2014-4).

* corresponding author: `Franck.Celestini@unice.fr`

[1] P.-G. de Gennes, F. Brochard-Wyart and D. Quéré, *Cap-*

illarity and wetting phenomena: drops, bubbles, pearls, waves (Springer New York, 2004).
[2] M. K. Chaudhury, and G. M. Whitesides, Science 256, 1539 (1992).
[3] F. D. Dos Santos, and T. Ondarçuhu, Phys. Rev. Lett. 75, 2972 (1995).
[4] Y. Sumino, N. Magome, T. Hamada, and K. Yoshikawa, Phys. Rev. Lett. 94, 068301 (2005).
[5] A. Frohn and N. Roth, *Dynamics of droplets* (Springer Berlin Heidelberg, 2000).
[6] H. Lamb, *Hydrodynamics* (Cambridge University press, 1932).
[7] S. Daniel, M. K. Chaudhury, and P.-G. de Gennes, Langmuir 21, 4240 (2005).
[8] X. Noblin, R. Kofman, and F. Celestini, Phys. Rev. Lett. 102, 194504 (2009).
[9] P. Brunet, J. Eggers, and R. D. Deegan, Phys. Rev. Lett. 99, 144501 (2007).
[10] J. G. Leidenfrost, *De Aquae Communis Nonnullis Qualitatibus Tractatus* (Duisburg on Rhine, 1756).
[11] D. Quéré, Annu. Rev. Fluid Mech. 45, 197 (2013).
[12] H. Linke, B. J. Alemàn, L. D. Melling, M. J. Taormina, M. J. Francis, C. C. Dow-Hygelund, V. Narayanan, R. P. Taylor, and A. Stout, Phys. Rev. Lett. 96, 154502 (2006).
[13] D. Vollmer , and H.-J. Butt, Nature Physics 10, 475 (2014).
[14] D. Richard, C. Clanet, and D. Quéré, Nature 417, 811 (2002).
[15] J. B. Boreyko, and C.-H. Chen, Phys. Rev. Lett. 103, 184501 (2009).
[16] C. Clanet, C. Béguin, D. Richard, and D. Quéré, J. Fluid Mech. 517, 199 (2004).
[17] T. Darmanin, and F. Guittard, J. Am. Chem. Soc. 131, 7928 (2009).
[18] G. Ramos Chagas, X. Xie, T. Darmanin, K. Steenkeste, A. Gaucher, D. Prim, R. Méallet-Renault, G. Godeau, S. Amigoni, and F. Guittard, J. Phys. Chem. C 120, 7077 (2016).
[19] See Supplemental Material at xxxx for the movies M1, M2, M3 and M4.
[20] L. D. Landau and E. M. Lifshitz, *Theory of Elasticity, Vol. 7 of Course of Theoretical Physics* (2nd english ed., Pergamon, 1970).